Journal of Chemical Crystallography
https://doi.org/10.1007/s10870-022-00940-6

ORIGINAL PAPER

Hydrothermal Single Crystal Growth and Structural Investigation of the Nepheline and Kalsilite Stuffed Tridymite Species

Rylan J. Terry[1,2] · Colin D. McMillen[1,2] · Joseph W. Kolis[1,2,3]

Received: 3 September 2021 / Accepted: 14 March 2022

Abstract

A series of high-quality single crystals of the formula $Na_xK_{1-x}AlSiO_4$ were synthesized using a high temperature hydrothermal method. This enabled the detailed single crystal study of four examples of this class of compounds, namely $KAlSiO_4$, $Na_{0.10}K_{0.90}AlSiO_4$ $Na_3KAl_4Si_4O_{16}$ and $NaAlSiO_4$. The potassium-containing species all had fully ordered AlO_4 and SiO_4 tetrahedral sites that led to formation of polar acentric structures. In contrast $NaAlSiO_4$ displayed the unusual feature of an exceptionally large and complex unit cell along with complete disordering of the Al and Si sites. This led to the formation of a centrosymmetric structure, that is also a new polymorph of the $NaAlSiO_4$ composition. The polymorphism of hydrothermal $KAlSiO_4$ was also examined in light of the crystal's synthetic and thermal histories. The study also revealed a structural sensitivity toward the degree of Na/K substitution in the lattice. The strong tendency to form polar acentric structures makes understanding these structures of great interest. These detailed structures resolved a considerable degree of previous structural ambiguity within this nominally simple class of compounds.

Graphical Abstract

Structural subtleties are examined in the nepheline–kalsilite series of $Na_xK_{1-x}AlSiO_4$, revealing changes in the resulting structure according to synthetic method, thermal history, and alkali metal substitution.

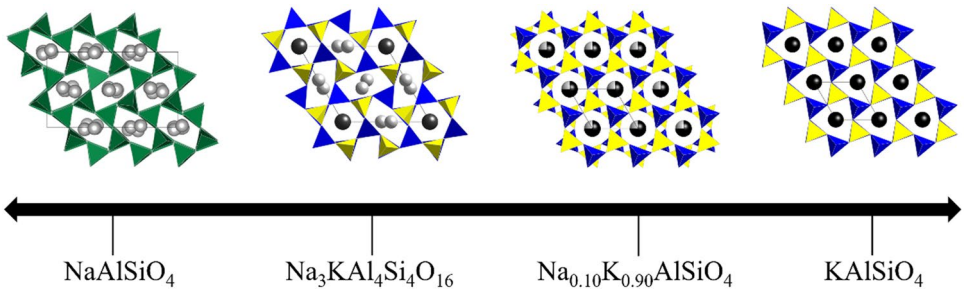

Keywords Hydrothermal synthesis · Silicate · Nepheline · Kalsilite

Introduction

The descriptive chemistry of the stuffed tridymite family has been shown to feature an interesting series of structural complexities.In its parent, highest symmetry hexagonal form, tridymite (SiO_2) is made up entirely of SiO_4 tetrahedra that form six-membered rings that link to each other in turn, forming layers in the *ab*-plane with hexagonal voids [1, 2]. The stuffed tridymite derivatives contain non-tetrahedral cations, typically alkali metals, within the

✉ Joseph W. Kolis
kjoseph@clemson.edu

[1] Department of Chemistry, Clemson University, Clemson, SC 29634-0973, USA

[2] Center for Optical Materials Science and Engineering Technologies (COMSET), Clemson University, Clemson, SC 29634-0973, USA

[3] 485 H.L. Hunter Laboratories, Clemson, SC 29634, USA

Published online: 26 March 2022

void spaces of the silicate rings. Such stuffed species not only exist in the tridymite family, but also in silica polymorphs such as quartz, keatite, and cristobalite [1, 3]. With the addition of a stuffing cation, a charge compensation must be made. Because of its relative crystallographic similarity to Si^{4+} and high terrestrial abundance, Al^{3+} often fulfills this charge compensating role through substitution of a Si^{4+} site in natural minerals leading to compositions such as $NaAlSiO_4$ and $KAlSiO_4$ for these stuffed tridymites. These types of minerals, which include nepheline and kalsilite, form a plethora of structures and formulas, not only on earth, but even in samples analyzed on Mars [4]. Despite the natural abundance of these materials, accurate structural determination is often challenging, and highly sensitive to subtle structural modifications, minute changes in chemical composition, thermal history, and origin. As a result, there is a wide range of structural variations within the $AAlSiO_4$ (A = Na, K) formulation (Table 1).

Table 1 Structural variations for compounds in the nepheline–kalsilite series

Composition	Space group	*a* (Å) α (°)	*b* (Å) β (°)	*c* (Å) γ (°)	Source	References
$NaAlSiO_4$	$P6_3$	9.958 90	9.958 90	8.341 120	Flux, 1100 °C	[5]
$NaAlSiO_4$	$P2_1$	17.23 90	25.06 119.75	27.23 90	Flux	[6]
$NaAlSiO_4$	$Pna2_1$	8.660 90	14.940 90	25.140 90	HT/HP Hydrothermal	[7]
$NaAlSiO_4$	$P2_1/n$	8.589 90	8.146 89.89	15.033 90	HT/HP Hydrothermal	[7]
$NaAlSiO_4$	$P6_1$	10.046 90	10.046 90	25.140 120	HT/HP Hydrothermal	[8]
$NaAlSiO_4$	Pn	14.991 90	8.625 90.2	25.110 90	HT/HP Hydrothermal	[9]
$NaAlSiO_4$	$P6_1$	9.995 (2) 90	9.995 (2) 90	24.797 (4) 120	Flux, 1100 °C	[10]
$Na_{7.85}Al_{7.85}Si_{8.15}O_{32}$	$P112_1$	9.9897 (6) 90	9.9622 (6) 90	24.979 (2) 119.788 (4)	Flux, 1150 °C	[11]
$NaAlSiO_4$	$P2_1/n$	14.9612 (7) 90	8.6234 (4) 90.133 (2)	25.1167 (12) 90	HT/HP Hydrothermal	This work
$Na_{4-x}K_xAl_4Si_4O_{16}$	$P6_3$	9.9774 (2) 90	9.9774 (2) 90	8.3634 (2) 120	Volcanic Mineral	[12]
$Na_{3.48}K_{0.48}Al_{3.96}Si_{4.04}O_{16}$	$P6_3$	9.989 (3) 90	9.989 (3) 90	8.380 (5) 120	Flux, 1100 °C	[13]
$Na_3KAl_4Si_4O_{16}$	$P6_3$	10.0155 (2) 90	10.0155 (2) 90	8.3944 (4) 120	HT/HP hydrothermal	This work
$Na_{0.283}K_{0.717}AlSiO_4$	$P6_3$	20.496 (5) 90	20.4969 (5) 90	8.549 (3) 120	Volcanic Mineral	[14]
$Na_{0.10}K_{0.90}AlSiO_4$	$P6_3$	5.1543 (7) 90	5.1543 (7) 90	8.6927 (17) 120	HT/HP Hydrothermal	This work
$KAlSiO_4$	$P31c$	5.1636 (3) 90	5.1636 (3) 90	8.7179 (6) 120	HT/HP Hydrothermal	this work
$KAlSiO_4$	$P31c$	5.157 (1) 90	5.157 (1) 90	8.706 (3) 120	Metamorphic Mineral	[15]
$KAlSiO_4$	$P6_3$	5.151 (5) 90	5.151 (5) 90	8.690 (8) 120	HT/HP Hydrothermal	[16]
$KAlSiO_4$	$P6_3$	5.1666 (1) 90	5.1666 (1) 90	8.7123 (1) 120	Hydrothermal, 300 °C	[17]
$KAlSiO_4$	$P6_3mc$	5.153 (5) 90	5.153 (5) 90	8.682 (9) 120	Alkali exchange	[18]
$KAlSiO_4$	$P2_1$	15.669 (2) 90	9.057 (1) 90.16 (1)	8.621 (1) 90	Dry synthesis	[19]
$KAlSiO_4$	$P6_3$	18.1111 (8) 90	18.1111 (8) 90	8.4619 (4) 120	Volcanic Mineral	[20]

The synthetic pursuit of tridymites dates back to the late 1800s in the gold lined autoclaves of von Chroustshoff [21] A key current interest in pursuing synthetic studies of stuffed tridymites lies in their tendency to crystallize in noncentrosymmetric (NCS) space groups, which often result in interesting physical and optical properties, including piezoelectric behavior and second harmonic generation [22, 23]. Indeed, during WWII, the synthesis of acentric nepheline, $NaAlSiO_4$, was pursued as an alternative to quartz in Germany, due to the high demand brought on by the embargo of high purity of quartz from Brazil [24–26]. It is statistically rare for a material to crystallize without a center of symmetry, with only about 13% of known inorganic structures lacking an inversion center [27]. Certain classes of compounds break this tendency to varying degrees. For example, borates, comprised of trigonal planar and tetrahedral building blocks (which themselves lack a center of symmetry), have been reported to have a nearly threefold greater tendency to crystallize without a center of symmetry [27]. While the aluminosilicates lack the ability to form trigonal planar oxo groups, it has been demonstrated that NCS arrangements of tetrahedral oxides, such as those containing $(AlO_4)^{5-}$ and $(SiO_4)^{4-}$ oxyanions, are also favorable [22]. Furthermore the ability to stack the tetrahedra also makes for a high tendency of *polar* acentric crystals. It can be noted that of the 21 reported structural examples of sodium and potassium stuffed tridymites listed in Table 1, 19 are polar acentric, a ratio far above other material categories to our knowledge. In this regard, the stuffed tridymites in the nepheline and kalsilite systems provide an excellent test bed for studying the design and physical properties of acentric and polar structures, as subtle compositional and synthetic factors may drive the parent centrosymmetric (CS) structure into one of the lower symmetry NCS modifications. Structural variations include ordering of the tetrahedral sites, distortion of the six-membered rings that form the structures, eclipsed orientation of the tetrahedra between layers, and variations in the orientation of the tetrahedra with respect to the *c*-axis [1, 3]. These variations in the aluminosilicate network are often influenced by changes in the size and composition of the stuffed alkali metals. In some instances, the structural perturbations result in larger unit cells, such as is the case in trinephelines, where an expansion of the cell along the *c*-axis is required to accommodate the orientation of the layers on the *ab*-plane [6, 10, 11].

Given the numerous structural variations reported in the $NaAlSiO_4$–$KAlSiO_4$ system (Table 1), we sought to apply a high temperature hydrothermal synthetic approach to examine how this synthetic approach affects the structures that are formed, and within this approach, how compositional factors further influence phase formation. This method is particularly useful in this system, because it offers a closed reaction with stoichiometric control, is well-known to be amenable to a wide variety of silicates, and often produces large, high quality single crystals [28–33]. The synthetic hydrothermal conditions may also approximate some conditions under which these phases form in nature, and thus the resulting structures may provide a useful frame of reference for understanding the formation of natural samples and identify conditions which preferentially stabilize certain polymorphs. Herein we explore the synthetic and structural aspects of a series of $Na_xK_{1-x}AlSiO_4$ compounds synthesized via a high-temperature, high-pressure hydrothermal technique.

Experimental

Synthesis

Single crystals of the $Na_xK_{1-x}AlSiO_4$ series were synthesized via hydrothermal reaction of 0.05 g (0.83 mmol) SiO_2 (Strem, 98%) and 0.042 g (0.415 mmol) Al_2O_3 (Alfa Aesar, 99.5%). To aid crystallization and act as the alkali nutrient source, a mineralizer fluid of 0.4 mL of a 10 M *A*OH (*A* = Na, K) was used. The stoichiometry of the mineralizers was controlled accordingly to achieve the desired alkali metal content in the final products. The powders and mineralizer solutions were placed within silver ampoules, 2.5 in. in length with an OD of 3/8 in. and welded shut at both ends. These ampoules were then loaded into a Tuttle cold seal autoclave, with the remaining volume filled with water to serve as the counterpressure. The reactions were heated at 650 °C and 200 MPa for 7 days. After cooling the autoclave to room temperature, the resulting crystals were washed with deionized water and allowed to air dry. Crystals produced by this method with a greater sodium content possessed a hexagonal column-shaped habit with sizes as large as 1.0 mm in length and 0.2 mm in diameter. As potassium was substituted in the place of sodium a hexagonal plate-like habit was observed, with sizes as large as 3 mm in diameter and 0.3 mm in thickness.

Structure Determination

A summary of the crystallographic data for $Na_xK_{1-x}AlSiO_4$ series is provided in Table 2. Single crystal X-ray diffraction was performed on a Bruker D8 Venture equipped with an Incoatec Mo Kα (λ = 0.71073 Å) microfocus source and Photon 100 CMOS detector. All data were collected at room temperature using phi and omega scans. Data collection, processing, and scaling were performed using Apex3 [34]. Data collection strategies yielded a multiplicity of observations exceeding ten in all structures. The structures were solved by direct methods and refined by full-matrix least-squares on F^2 using the SHELXTL software suite [35]. All atoms were

Table 2 Crystallographic data for the hydrothermally-grown $Na_xK_{1-x}AlSiO_4$ series

Empirical formula	$KAlSiO_4$	$Na_{0.10}K_{0.90}AlSiO_4$	$Na_3KAl_4Si_4O_{16}$	$NaAlSiO_4$
Formula weight (g/mol)	158.17	156.56	584.35	142.06
Space group	*P*31*c*	$P6_3$	$P6_3$	$P2_1/n$
a (Å)	5.1636 (3)	5.1543 (7)	10.0155 (2)	14.9612 (7)
b (Å)	–	–	–	8.6234 (4)
c (Å)	8.7179 (6)	8.6927 (17)	8.3944 (4)	25.1167 (12)
β (°)	–	–	–	90.133 (2)
Volume ($Å^3$)	201.33 (7)	200.00 (7)	729.23 (5)	3240.5 (3)
Z	2	2	2	36
Density (calculated) (g/cm^3)	2.609	2.600	2.661	2.621
Parameters	24	23	93	573
θ range (°)	4.56–28.18	4.57–25.15	2.35–26.00	2.12–28.00
Reflections				
Collected	1950	1724	8375	170,082
Independent	331	248	969	7823
Observed, $I \geq 2\sigma(I)$	312	217	904	7566
R, int	0.0267	0.0359	0.0385	0.0506
Final R, obs. data				
R1	0.0189	0.0339	0.0204	0.0378
wR2	0.0447	0.0832	0.0445	0.1050
Final R, all data				
R1	0.0205	0.0386	0.0235	0.0392
wR2	0.0452	0.0857	0.0456	0.1056
Goodness of fit of F^2	1.178	1.259	1.064	1.277

refined anisotropically. The structure of $KAlSiO_4$ was refined as an inversion twin, having an absolute structure parameter of 0.40(3). The NCS nature of $KAlSiO_4$, $Na_{0.10}K_{0.90}AlSiO_4$, and $Na_3KAl_4Si_4O_{16}$ was verified by observation of second harmonic generation, with Flack parameters supporting the correct absolute structure. The structure of $Na_3KAl_4Si_4O_{16}$ was additionally refined as a merohedral twin with a batch scale factor of 0.41. The structure of $NaAlSiO_4$ was refined as a pseudo-merohedral twin with a batch scale factor of 0.19. Figures of the crystal structures were drawn using VESTA [36]. Structural data have been deposited with the joint CCDC/FIZ Karlsruhe deposition service, deposition numbers 2106945–2106948. Verification of the structures and phase purity was made by powder X-ray diffraction (PXRD) performed using a Rigaku Ultima IV diffractometer with Cu Kα radiation (λ = 1.5406 Å) at 0.02° intervals at a rate of 1°/min from 5 to 65°.

Additional Characterization

Elemental analysis of the crystals used for structural analysis was carried out using energy dispersive X-ray analysis (EDX). To perform these measurements, a Hitachi S-3400N scanning electron microscope (SEM) equipped with an Oxford INCA EDX detector was employed. Crystals selected for analysis were attached to a carbon disc using double-sided carbon tape. This disc was then placed onto a 51 mm stage that was then placed into the SEM chamber. After the chamber was evacuated, the electron beam was activated with an acceleration voltage of 20 kV. Measurements taken in this fashion were completed as an average of multiple measurements over a selected flat region of each crystal.

The structural phase transformation behavior of $KAlSiO_4$ was studied using differential scanning calorimetry (DSC). These measurements were performed using a TA Instruments SDT Q600 DSC/TGA. Powdered samples of the analyte were placed in an alumina crucible, along with an empty reference sample pan. The heating profile for the study proceeded from 25 to 1000 °C at a rate of 10 °C/min in a nitrogen atmosphere.

Results and Discussion

The Crystal Structure of $KAlSiO_4$

The stuffed tridymite structural family contains a number of structural transitions, caused often by only very minor changes in their formulaic composition or synthetic route. There is perhaps no greater example of this than in the $Na_xK_{1-x}AlSiO_4$ series. Depending on the ratio of sodium

to potassium ions within the same aluminosilicate framework, four distinct phases are observed in the present study of hydrothermally-grown crystals. Although these alkali ions only have a radius difference of 0.25 Å, the change has a remarkable effect on the structural framework.

The mineral kalsilite, $KAlSiO_4$, is the largest end member of this series and is most commonly observed in the hexagonal setting of $P6_3$ [1, 37, 38], while some samples from southern India have been found to occur in the trigonal setting of $P31c$ [15]. The two key differences between the occurrence of these polymorphs is the environment in which they are formed and the amount of sodium impurities reported within the crystal. The hexagonal phase is predominantly found in volcanic rocks or with a minor amount of sodium impurities in metamorphic rocks. The trigonal specimens have been found in metamorphic granulite facies gneiss with nearly no sodium contamination. Synthesis of $KAlSiO_4$ by traditional solid-state methods is known to produce the hexagonal phase [16]. However, when crystalized under hydrothermal conditions in the present study (650 °C, 10 M KOH), the trigonal phase is produced exclusively, yielding an excellent refinement (R1 = 0.0189) in $P31c$ (Table 2).

A useful way to understand the differences between the various polymorphs of $Na_xK_{1-x}AlSiO_4$ is to compare the aluminosilicate framework to that of high tridymite. In each of this series, small distortions in the framework reduce the symmetry to variety of unique structures. An illustration of these changes in presented in Fig. 1.

In trigonal $KAlSiO_4$ specifically, the symmetry is reduced from the ideal tridymite $P6_3/mmc$ to $P31c$ by the ordering of the tetrahedral cations and by the way in which the tetrahedra connect to one another within the *ab*-plane. The AlO_4 and SiO_4 tetrahedra that form the aluminosilicate framework of this structure are built up of layers of ditrigonal six-membered rings parallel to the *ab*-plane, where the orientations of threefold axes of the neighboring tetrahedra are alternating up and down along the *c*-axis. The potassium ions reside in the channels, hence the "stuffed" terminology (Fig. 2). These layers are then connected to one another along the *c*-axis by the O_1 atom bridging the Si_1 atom of one layer with the Al_1 atom of the next layer, thereby creating channels formed by the six membered rings in all three principal axes (Fig. 3). The orientation of the all the SiO_4 tetrahedra along the *c*-axis and all of the AlO_4 tetrahedra along *c* establish the polar axis. Importantly, the basal oxygen atoms of the bridged tetrahedra are eclipsed along the *c*-axis in the $P31c$ setting of $KAlSiO_4$ (Fig. 2a), whereas they are staggered in the $P6_3$ setting (Fig. 2b). In the trigonal structure here, the three basal oxygen atoms for each of the SiO_4 and AlO_4 tetrahedra are accounted for by one unique oxygen site. The average Si–O and Al–O bond distances are 1.647(12) Å and 1.700 (12) Å, respectively, as is typically expected [39].

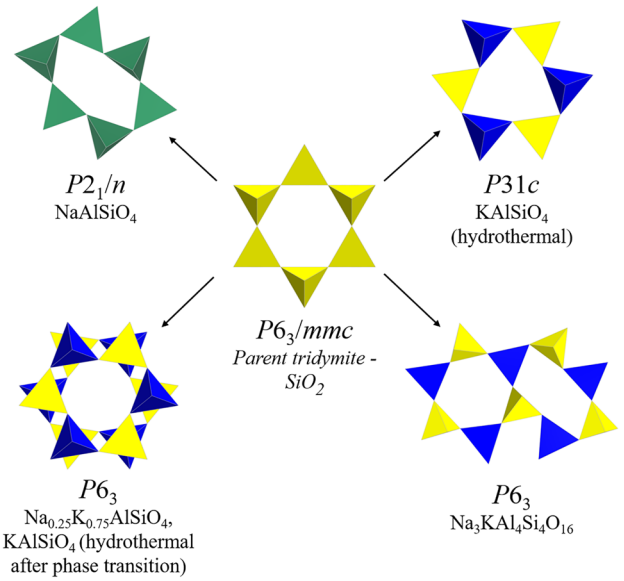

Fig. 1 Structural modifications of the tridymite framework as seen in the hydrothermal $Na_xK_{1-x}AlSiO_4$ series. Yellow tetrahedra represent SiO_4 groups, blue represents the AlO_4 groups, and green represent disorder between the two (Color figure online)

Since the majority of the literature reports for natural $KAlSiO_4$ are in the hexagonal setting, and given the similarity between these space groups, a test refinement was performed on our synthetic crystals in $P6_3$. This solution led to a less desirable R-value (0.0599), disorder of the basal oxygen sites, and poor anisotropic displacement parameters in the $P6_3$ setting (Supporting Information, Table S1). This is related to the eclipsed nature of the trigonal structure versus the staggered arrangement of the hexagonal structure, as illustrated in Fig. 2. A prior study of $KAlSiO_4$ prepared hydrothermally at 600 °C and 14 kpsi suggested a disordered structure in space group $P6_3$ having a high R1 value of 0.084 [16], with the disordered domains giving the appearance of $P6_3mc$ symmetry. Indeed, $P6_3$ crystals have been thermally converted to the $P6_3mc$ structure at 865 °C, and the $P6_3mc$ structure verified at 950 °C [40]. Naturally-occurring kalsilite having $P31c$ symmetry has been thermally converted to $P6_3$ symmetry at 500 °C [41]. This is interesting since the present synthetic study was performed at 650 °C, and yet the $P31c$ structure was isolated in good crystalline quality. Thus, we were interested to study the thermal behavior of these metastable $P31c$ crystals having this specific hydrothermal synthetic history.

The DSC measurements (Fig. 4) indicate a single-phase transition occurring at 882 °C upon heating and 872 °C upon cooling, which is in agreement with a phase transition from $P31c \rightarrow P6_3mc$ upon heating. Purity of the material prior to heating was verified by PXRD (Fig. 5), and the absence of *hhl*, *l* = odd reflections combined with the single crystal

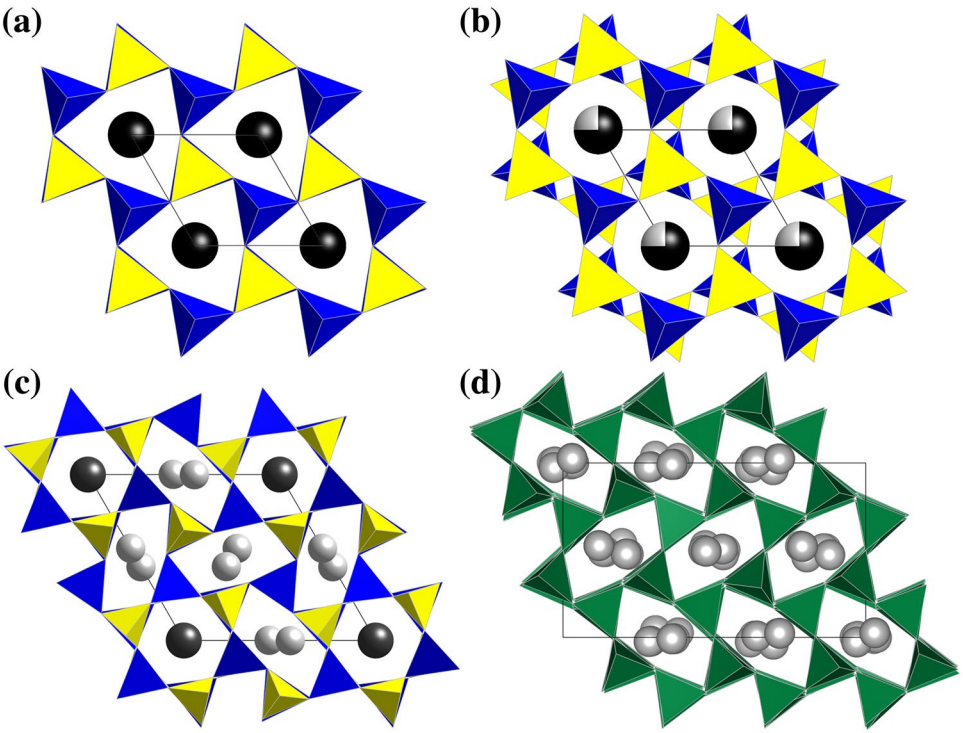

Fig. 2 Crystal structures of **a** $KAlSiO_4$ (hydrothermal), **b** $Na_{0.10}K_{0.90}AlSiO_4$ (and hydrothermal $KAlSiO_4$ after phase transition, where alkali ions would be all black, as pure K^+), **c** $Na_3KAl_4Si_4O_{16}$, and **d** $NaAlSiO_4$ as viewed down the *c*-axis. Yellow tetrahedra represent SiO_4 groups, blue represents the AlO_4 groups, and green represent disorder between the two. Silver atoms represent sodium and black atoms represent potassium (Color figure online)

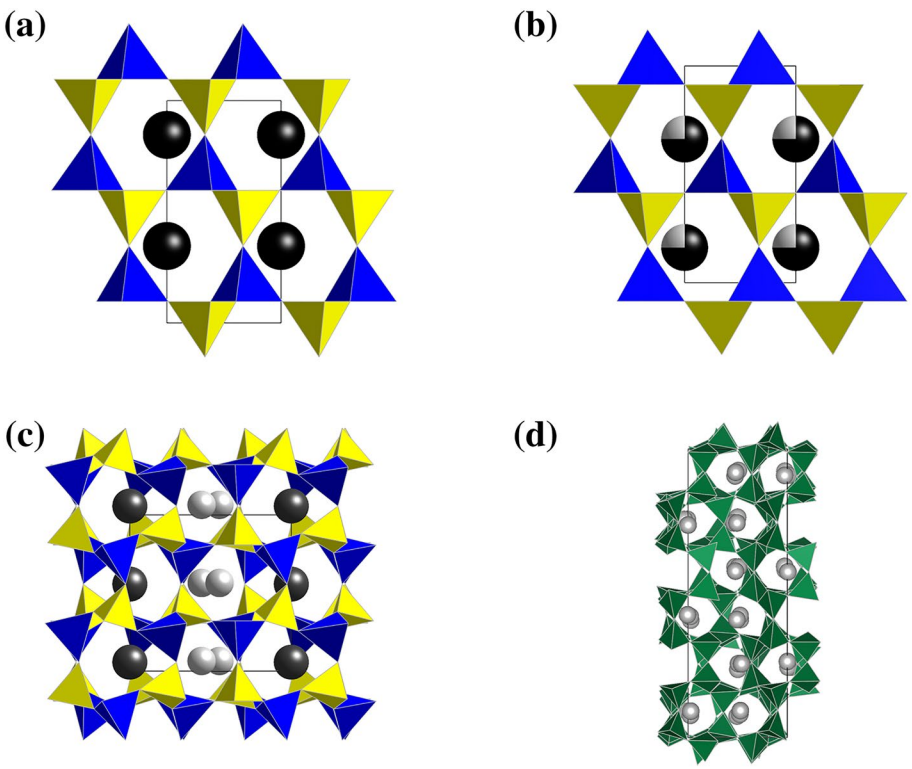

Fig. 3 Crystal structures of **a** $KAlSiO_4$ (hydrothermal), **b** $Na_{0.10}K_{0.90}AlSiO_4$ (and hydrothermal $KAlSiO_4$ after phase transition, where alkali ions would be all black, as pure K^+), **c** $Na_3KAl_4Si_4O_{16}$, and **d** $NaAlSiO_4$ as viewed down the *a*-axis. Yellow tetrahedra represent SiO_4 groups, blue represents the AlO_4 groups, and green represent disorder between the two. Silver atoms represent sodium and black atoms represent potassium (Color figure online)

measurements indicates the starting material was entirely $P31c$ prior to the phase transition. PXRD analysis of the same sample after cooling indicates that the phase transition is only pseudo-reversible, as the resultant material does not have $P31c$ symmetry, but instead has $P6_3$ symmetry, exhibiting the characteristic weak *hhl*, $l =$ odd reflections such as (111), (113), and (115). To verify this $P6_3mc \rightarrow P6_3$ transition upon cooling, we performed a single crystal structure

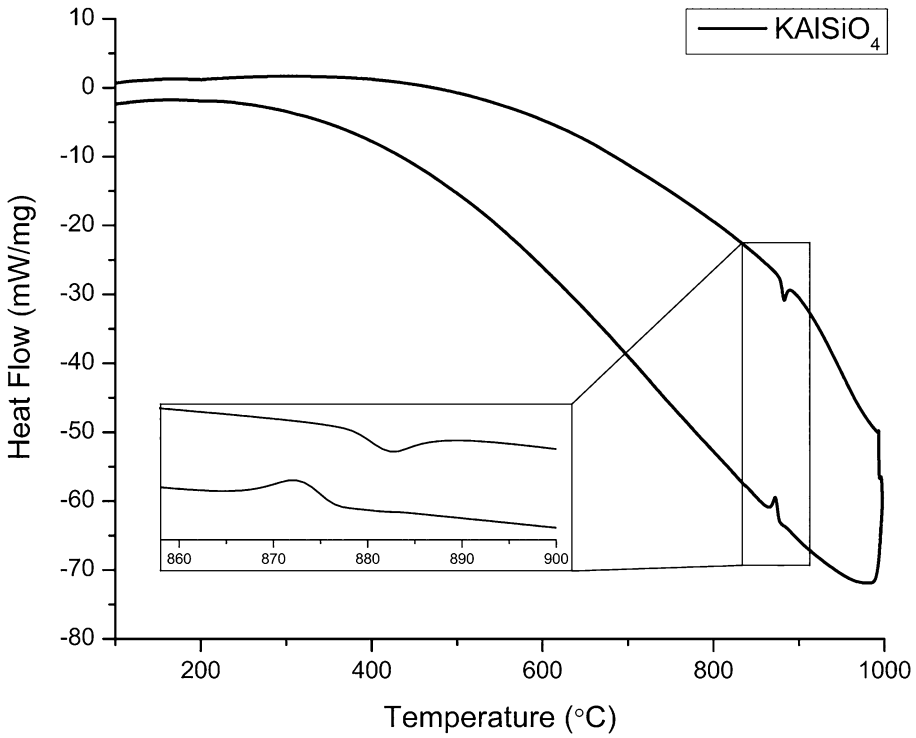

Fig. 4 DSC of hydrothermally-grown $KAlSiO_4$

analysis on a single crystal retrieved from the DSC experiment, and found it could be best refined in $P6_3$, with less satisfactory results in $P31c$ and $P6_3mc$ (SI, Table S2). The basal oxygen sites were found to be well-ordered, as is seen in other $P6_3$ examples of $KAlSiO_4$, while the basal oxygen sites of the $P31c$ and $P6_3mc$ test refinements were disordered and required restraints to prevent them from becoming non-positive definite. While it was clear that kalsilite structures were already sensitive to compositional and synthetic factors, it appears their thermal behavior is also influenced in subtle ways by the synthetic history of the samples. The $P31c$ kalsilites appear to be kinetically stable phases that may not be easily recovered once they have experienced thermal treatment.

The Crystal Structure of $Na_{0.10}K_{0.90}AlSiO_4$

As sodium ions are intentionally added to the reaction mixture in a 1:3 Na:K ratio under hydrothermal conditions, the common, naturally occurring hexagonal $P6_3$ phase of kalsilite is produced, albeit with substitutional disorder of Na/K ions. Single crystal X-ray diffraction data from the resultant crystals was refined as $Na_{0.10}K_{0.90}AlSiO_4$ in the polar acentric setting of $P6_3$ (Figs. 2b, 3b). While the size of the stuffing cation in $Na_{0.10}K_{0.90}AlSiO_4$ has been reduced by the partial substitution of smaller sodium into the potassium sites, the overall unit cell dimensions have only slightly decreased in comparison to $KAlSiO_4$. The significant difference between these two structures relates more to the structural arrangement of the tetrahedral framework. In trigonal $KAlSiO_4$ the aluminosilicate framework is coordinated in an eclipsed fashion with respect to the c-axis. In hexagonal $Na_{0.10}K_{0.90}AlSiO_4$, however, the tetrahedra are rotated into a staggered conformation. The difference in the K–O bond lengths of $P31c$ kalsilite versus the K/Na–O bond lengths of $P6_3$ kalsilite, is nearly negligible (SI, Tables S3, S4), and it appears the sodium ion is allowed greater mobility within the cation site, as the potassium ions present in the majority prevent the channels from becoming too narrow. To account for this change, the framework must twist from an eclipsed conformation to a staggered one to maintain a minimal coordination distance to the countercharging alkali. An illustration of the alkali site coordination in $Na_{0.10}K_{0.90}AlSiO_4$ and $KAlSiO_4$ is provided in Fig. 6.

Due to the similarities of the hexagonal setting of $P6_3$ and the trigonal $P31c$, a test refinement of $Na_{0.10}K_{0.90}AlSiO_4$ was performed in $P31c$. This test refinement led to an unfavorable solution with an R1 value of 0.0980. This poor solution is brought about by the same line of reasoning as to why $KAlSiO_4$ could not be reasonably solved in $P6_3$. In the trigonal solution, the basal oxygen sites are not repeated in a staggered fashion so an additional oxygen site must be added in $P31c$ to ensure a staggered solution, with both basal oxygen sites partially disordered. A test refinement was also performed in space group $P6_322$, to distinguish the true symmetry in $P6_3$ from $P6_322$ pseudosymmetry. The test case again produced a less favorable refinement (R1 = 0.0717).

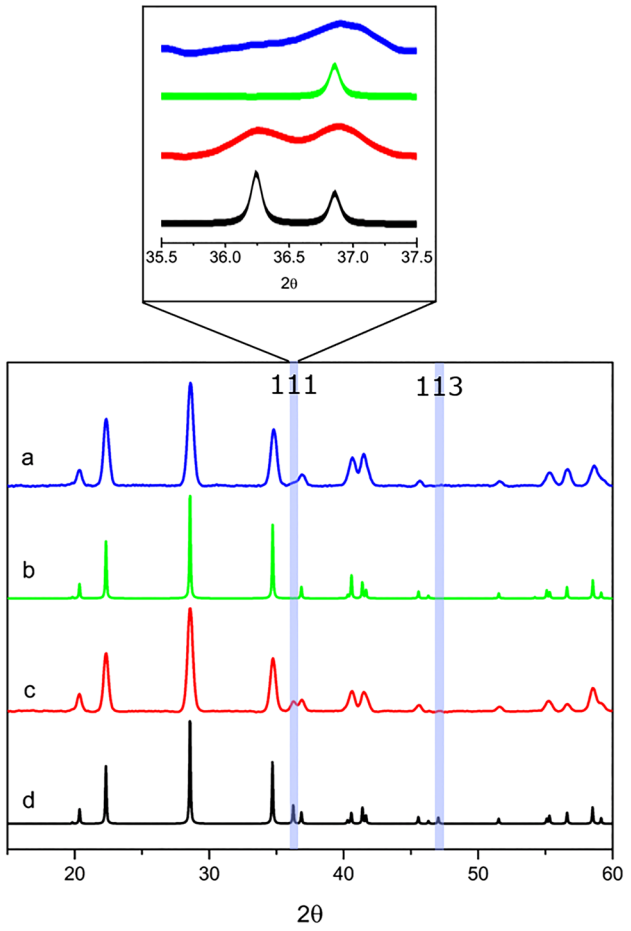

Fig. 5 PXRD of (a) hydrothermally-grown *P*31*c* $KAlSiO_4$, (b) calculated *P*31*c* $KAlSiO_4$, (c) experimental $P6_3$ $KAlSiO_4$ after cooling from thermal conversion at 882 °C, and (d) calculated $P6_3$ $KAlSiO_4$

The tetrahedra that make up the framework of $Na_{0.10}K_{0.90}AlSiO_4$ are slightly distorted. In these tetrahedra the basal oxygen atoms are distorted away from one another leading to O–T–O (T = Si or Al) angles of 111.0 (6)° for aluminum and 110.9 (6)° for silicon, while the angles between the apical oxygen atoms and the basal ones are slightly smaller at 107.9 (6)° for aluminum and 108.0 (6)° for silicon. This in turn also effects the bond lengths within the tetrahedra. The basal oxygen atom bonds are at 1.672 (7) Å and 1.670 (7) Å for Al and Si, respectively, though distinction between the sites can be made from their respective bond distances to the apical oxygen, at 1.69 (4) Å for aluminum and 1.63 (4) Å for silicon.

The Crystal Structure of $Na_3KAl_4Si_4O_{16}$

With an increase of the sodium to potassium ratio in the reaction mixture, the phase we designate as $Na_3KAl_4Si_4O_{16}$ is stabilized. This phase was stabilized from a number of reactions, ranging from the stoichiometric 3:1 sodium to potassium ratio all the way to a 1:1 ratio. The structure of the $Na_3KAl_4Si_4O_{16}$ phase is that of ideal nepheline in $P6_3$. Although it crystallizes in the same space group as $Na_{0.10}K_{0.90}AlSiO_4$, it is a structurally distinct entity with different lattice parameters and ordered Na and K sites [12, 42–46]. Variations in naturally occurring nephelines can lead to disorder of the aluminum and silicon sites [42, 43], as well as potassium-poor stoichiometries [12, 46]. Like other stuffed tridymite derivatives, the structure is built of six membered rings composed of SiO_4 and AlO_4 tetrahedra. In the synthetic hydrothermal material we find the aluminum and silicon sites to be well ordered [and clearly distinguishable based on Al–O bond lengths of 1.71 (2) Å to 1.753 (8) Å and Si–O bond lengths of 1.608 (8) to 1.63 (2) Å; SI Table S5], connecting in an alternating manner with respect the silicon and aluminum sites as well as the orientation of their tetrahedra with respect to the *c*-axis.

Similar to *P*31*c* kalsilite, subsequent layers of tetrahedra are eclipsed. Where this nepheline type structure sets itself apart from the other structures discussed thus far is the presence of two distinct ring types (Fig. 2c). The ring about the origin of the cell forms a nearly perfect hexagon when viewed down the *c*-axis, as it resides on the 6_3-screw axis. The second ring type of the framework is an oval ring. These rings develop along the *a* and *b* cell edges and at the center of the cell, filling the spaces adjacent and diagonal to the hexagonal ring types. Connectivity of the ring layers into the framework occurs via T–O–T angles of 137.8 (2)° and 156.5 (8)° for Si_1–O_2–Al_1 and Si_2–O_5–Al_2, respectively.

The structural motif is directed by the composition of two distinct alkali cations acting to charge balance the tetrahedral ring structures, with the ordered K^+ and Na^+ cations located in specific channels. The sodium ions are positioned in the center of the oval-shaped six-member rings, with an average Na–O bond length of 2.672 Å, and the potassium ions are located within the hexagonal rings, with an average K–O bond length of 3.004 Å. The environment of the oval ring is ideal for the smaller sodium ions and resists any tendency for potassium ion disorder at the sodium sites. It is consistent with the observation that synthesis of potassium-rich species having this structure type could not be obtained in our hands, leading instead to the formation of the $Na_{0.10}K_{0.90}AlSiO_4$ hexagonal kalsilite type phase, as well as the common occurrence of potassium-poor, but not potassium-rich natural nepheline samples. The 3:1 Na:K ratio of the synthetic samples, including the one used for the structure refinement, were confirmed by EDX.

The Crystal Structure of $NaAlSiO_4$

Hydrothermal synthesis using NaOH exclusively as the mineralizer solution led to a new polymorph of $NaAlSiO_4$. The seemingly simple formula of $NaAlSiO_4$ belies a variety of

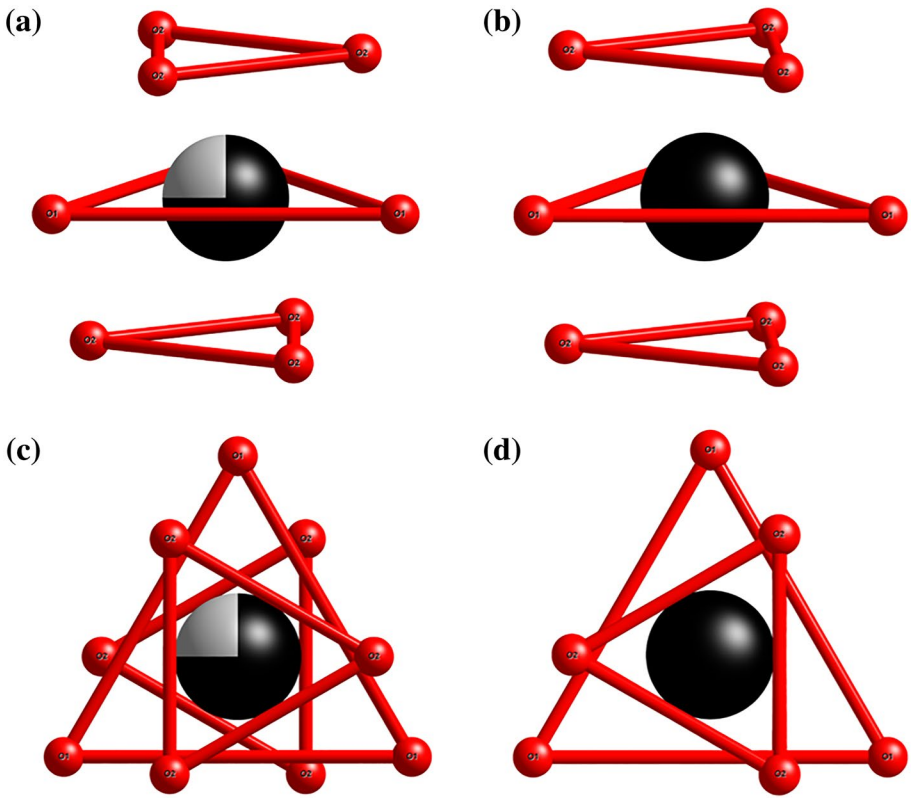

Fig. 6 Alkali metal ion environments in $Na_{0.10}K_{0.90}AlSiO_4$ (**a**, **c**) and $KAlSiO_4$ (**b**, **d**)

crystallographic determinations reported in the literature that are surprisingly convoluted [5–11, 47–49]. Prominent among these are a complex series of structures called the trinephelines, where the tetrahedral layers consist of exclusively oval-shaped channels. In the hexagonal ($P6_1$) trinepheline (Fig. 7), the aluminum and silicon sites are ordered, and subsequent layers are rotated as they are stacked along the extended *c*-axis [10]. This gives the appearance of hexagonal channels in the same locations as those in nepheline, though it is accomplished in this different manner of overlapping oval rings. There have also been a series of orthorhombic and monoclinic trinephelines reported in the literature [7, 9, 11]. They appear to be related to one another on the basis of their lattice parameters, but their refinements are somewhat ambiguous. Selker and coworkers reported several examples with the same formula that were refined in the NCS space groups *Pn* and $P2_1$ [9].

In this study we isolate a centrosymmetric (CS) modification in space group $P2_1/n$, whereby all the tetrahedral sites contain Al/Si disorder (SI, Tables S6, S7, S8, S9). These crystals were prepared by a similar method to that of Selker and have very similar unit cell constants. The absence of any second harmonic generation in the present sample, however, is consistent with a CS model. The beta angle very near 90° may also be the source of the apparent ambiguity regarding some of the previous assignments of orthorhombic symmetry [9, 11]. Indeed, the crystals here are subject to pseudo-merohedral twinning that often suggests higher symmetry. An apparent hexagonal unit cell of a = 17.25, c = 25.12 was often obtained during indexing, but a reasonable solution was not obtained with these parameters. Ultimately, the monoclinic unit cell of $a = 14.9612$ (7), $b = 8.6234$ (4), $c = 25.1167$ (12), $\beta = 90.133$ (2) was achieved (itself very close to orthorhombic metric symmetry), where the *b*-axis is half of the apparent hexagonal *a*-axis. Axial photographs (Fig. 8) confirmed the apparent hexagonal *a*-axis was due to a sparse row of reflections found along the true *b*-axis and was accounted for by a 20% twin fraction of the pseudo merohedral twin of twofold rotation about the *c*-axis.

An important departure occurs in the tetrahedral framework of the CS monoclinic polymorph relative to that of the of the NCS trinepheline in the $P6_1$ structure. In the monoclinic polymorph of the present study, the aluminum and silicon atoms are substitutionally disordered across all the tetrahedral sites. The Si/Al-O bonds range from 1.6570 (10) to 1.696 (3) Å, intermediate of typical Si–O and Al–O bond lengths. The substitutional disorder persisted in test refinements in lower symmetry space groups. The individual aluminosilicate layers adopt similar oval-shaped channels to those in trinepheline, but there is no incremental rotation of consecutive layers as the layers stack along the *c*-axis as there is from the 6_1 screw axis of trinepheline. Thus there are no nepheline-like hexagonal

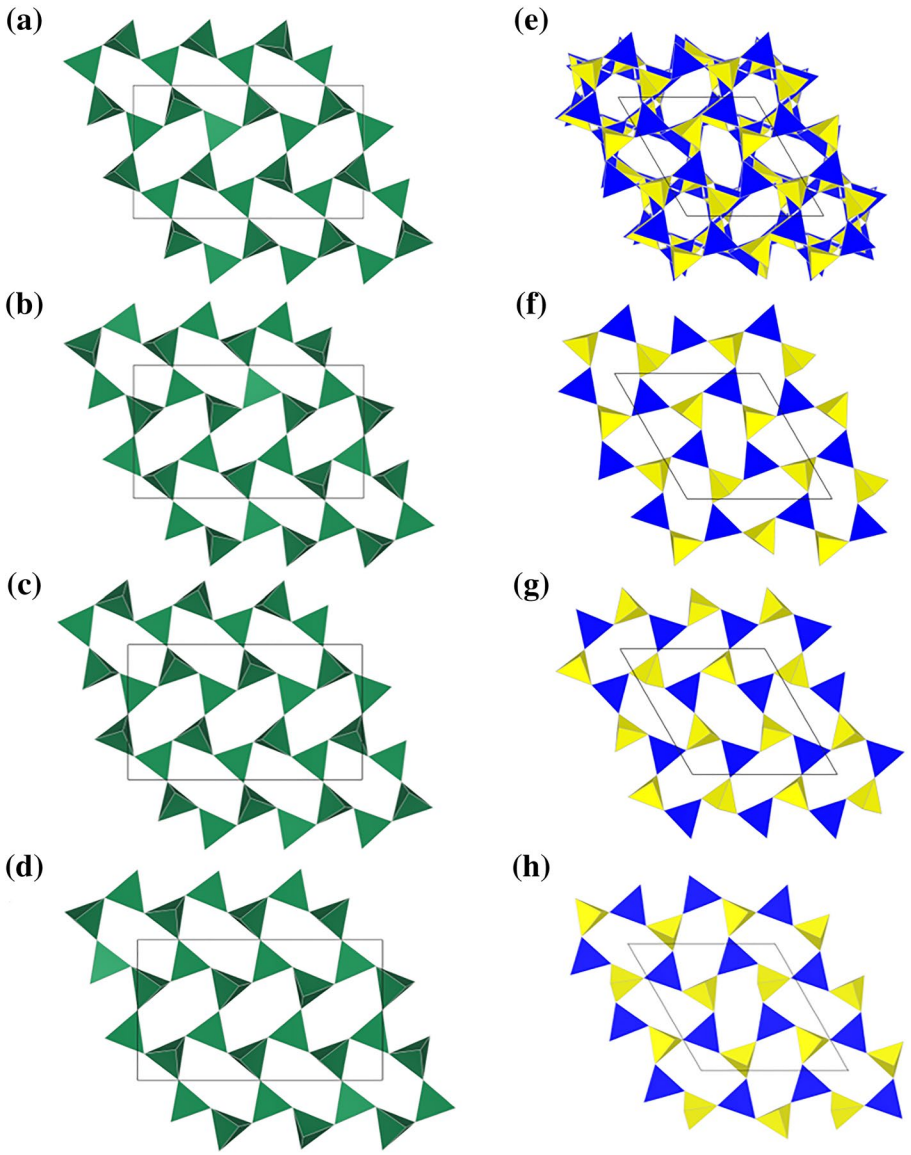

Fig. 7 **a**–**d** The layers of monoclinic trinepheline **a** $1.09 < z < 0.90$, **b** $0.92 < z < 0.75$, **c** $0.77 < z < 0.57$, and **d** $0.60 < z < 0.40$. **e** All layers of hexagonal trinepheline, **f**–**h** The layers of hexagonal trinepheline **f** $1.03 < z < 0.85$, **g** $0.87 < z < 0.68$, and **h** $0.70 < z < 0.52$ [10]. Green tetrahedra represent disordered sites between silicon and aluminum oxides, yellow tetrahedra represent SiO_4, and blue represents the AlO_4 groups (Color figure online)

channels that are formed in the long range structure of the monoclinic polymorph, where the oval shaped channels of the individual layers are aligned by the 2_1 screw axis. The ring coordination for the individual layers of hydrothermally synthesized $NaAlSiO_4$ is provided in Fig. 7a–d. At first glance these layers appear nearly identical, with only slight deviations in the positions of the basal oxygen atoms that connect the rings. These layers are very similar to those seen in hexagonal trinepheline (Fig. 7e–h) and is particularly obvious in the second layer (Fig. 7g). The similarity of the first and third layers (Fig. 7f, h) is not as immediately apparent due to their rotation caused by the hexagonal nature of the structure. As the rotation axis is reduced in symmetry from $P6_1$ to $P2_1/n$, minute differences from layer to layer necessitate the tripled *c*-axis of the $P2_1/n$ trinepheline. These layers are arranged in an ABCDCBA type fashion, with an inversion center at the center of the D-layer. In comparison, hexagonal trinepheline is layered in an ABCABC ordering.

The angles within the tetrahedra of $NaAlSiO_4$ do show some distortion from the ideal 109.5°, with angles ranging 104.31 (15)–115.88 (12)° (SI, Table S8). There does not appear to be any discernable pattern in these deviations and the averaging of all O–T–O angles within the tetrahedral are very close to 109.5° at all eighteen sites, however, the T–O–T angles provide some interesting information (SI, Table S9). In viewing the cell down the *c*-axis, most basal oxygen atoms within the cell are at both the corner of one of the 6-membered rings and along the flat section of its neighboring ring. However, this is not true for the oxygen atoms at one corner position of the rings. Along the *a*-axis of the cell, the oxygen atoms at the corner of

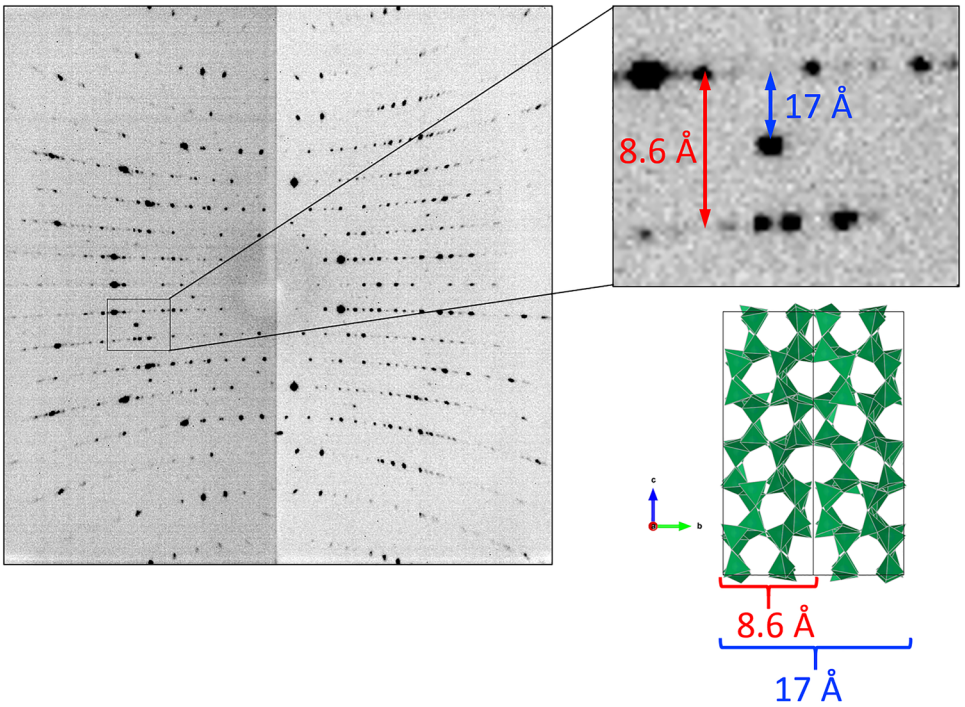

Fig. 8 *b*-Axial photograph of monoclinic trinepheline with the crystal structure of monoclinic trinepheline as viewed down the *a*-axis, as well as the twin of the cell, green tetrahedra represent disordered sites between silicon and aluminum oxides (Color figure online)

two neighboring rings have the largest T–O–T angles. In fact, for two specific oxygen atoms, O_{13} and O_{29}, these angles are exactly 180°. While such angles in silicates and aluminosilicates are unusual [50], there have been several examples of this occurring in the tridymite system [51, 52]. In the case of both sites this linear angle is required by symmetry as these oxygen atoms lie at inversion centers of the cell. There was no experimental evidence for the splitting of O_{13} and O_{29} off of the symmetry site, and only O_{29} showed any relative anisotropy when compared with other oxygen sites within the structure.

The key distinction from ideal nepheline [44], $Na_3KAl_4Si_4O_{16}$, is that this monoclinic trinepheline contains only Na^+ ions. This leads to the formation of only one general type of oval shaped aluminosilicate ring, compared to $Na_3KAl_4Si_4O_{16}$, where the larger K atoms templated hexagonal rings and the smaller Na toms templated oval-shaped rings. The rings of hydrothermal $NaAlSiO_4$ similarly contrast with those templated by mixed occupancy Na/K sites of $Na_{0.10}K_{0.90}AlSiO_4$ and the K sites of $KAlSiO_4$, where the larger potassium atoms led to ditrigonal rings. In monoclinic trinepheline the coordination environments of the Na^+ ions range from 8 to 11 coordinate at a maximum Na–O distance of 3.5 Å. The variation in coordination is due to the loose positioning within the channels and the nearly negligible stabilizing contribution of bonds at this maximum. Probably more important is the recurrence of 4 shorter Na–O distances at each of the Na sites. These distances were found to be as short as 2.290 (4) Å, making them ill-suited for a larger alkali metal such as K^+.

Summary and Conclusions

The nepheline–kalsilite ($NaAlSiO_4$–$KAlSiO_4$) system is a complicated series with interesting structural variations as a function of both composition and crystal growth conditions. Hydrothermal synthesis was used to access high quality crystals in the $K_{1-x}Na_xAlSiO_4$ system, in order to study these influences under common growth conditions. In the case of $KAlSiO_4$, hydrothermal conditions led to the less common trigonal polymorph in *P*31*c* with eclipsed ditrigonal rings. This is similar to metamorphic mineralogical samples but differs from samples of either volcanic origin or previous solid-state synthesis which form in $P6_3$ symmetry, having staggered ditrigonal rings that create hexagonal channels. DSC measurements suggested a phase transition from *P*31*c* to $P6_3mc$ upon heating to 882 °C, and then a phase transition from $P6_3mc$ to $P6_3$ at 872 °C upon cooling, suggesting the *P*31*c* form is a metastable form. Controlled introduction of Na into the hydrothermal system led directly to the hexagonal form of $Na_{0.10}K_{0.90}AlSiO_4$ in $P6_3$. Given the identical synthesis conditions to $KAlSiO_4$, the formation of staggered ditrigonal rings in $Na_{0.10}K_{0.90}AlSiO_4$ is attributed to the presence of sodium atoms in substitutional disorder with potassium. Further sodium substitution to produce $Na_3KAl_4Si_4O_{16}$ leads to an ordered arrangement of sodium and potassium atoms in the very different nepheline

structure type of space group $P6_3$. Alkali metal ordering templates the formation of distinct hexagonal and oval aluminosilicate rings in the framework. Hydrothermal synthesis in the absence of potassium led to the formation of a monoclinic form of trinepheline, $NaAlSiO_4$, which exhibits substitutional disorder of Al and Si atoms in $P2_1/n$. Refinement of high quality X-ray data accounting for pseudo merohedral twinning appears to resolve several uncertainties about monoclinic and orthorhombic trinephelines that are present in the older literature. The structure departs from that of the ordered hexagonal trinepheline, in that it maintains eclipsed oval-shaped channels throughout the framework and does not exhibit any of the hexagonal nepheline-like channels. The study demonstrates the utility of hydrothermal synthesis to systematically access compositions of interest in a controlled fashion to gain new insights into factors directing structural variations in complex systems. It is also clear that in the absence of tetrahedral oxyanion disorder, the likelihood of formation of polar acentric structures is very high due to the selective orientation of the Si/Al tetrahedra. This work may provide additional understanding of the factors leading to designed polar acentric crystals.

Supplementary Information The online version contains supplementary material available at https://doi.org/10.1007/s10870-022-00940-6.

Acknowledgements We are indebted to the National Science Foundation NSF-DMR1808371 for financial support of the synthesis and crystal growth.

Data Availability CCDC 2106945–2106948 contain the supplementary crystallographic data for this paper. These data can be obtained free of charge from The Cambridge Crystallographic Data Centre and FIZ Karlsruhe via www.ccdc.cam.ac.uk/data_request/cif. The authors declare that all other data supporting the findings of this study are available within the article and its Supplementary Information files.

Declarations

Conflict of interest CDM is an Associate Editor with Journal of Chemical Crystallography, and was excluded from the peer review process.

References

1. Palmer DC (1994) Stuffed derivatives of the silica polymorphs. Rev Mineral Geochem 29(1):83–122
2. Takada A, Glaser KJ, Bell RG, Catlow CRA (2018) Molecular dynamics study of tridymite. IUCrJ 5(3):325–334. https://doi.org/10.1107/S2052252518004803
3. Buerger MJ (1954) The stuffed derivatives of the silica structures. Am Mineral 39:600–614
4. Morris RV, Vaniman DT, Blake DF, Gellert R, Chipera SJ, Rampe EB, Ming DW, Morrison SM, Downs RT, Treiman AH, Yen AS, Grotzinger JP, Achilles CN, Bristow TF, Crisp JA, Marais DJD, Farmer JD, Fendrich KV, Frydenvang J, Graff TG, Morookian J-M, Stolper EM, Schwenzer SP (2016) Silicic volcanism on mars evidenced by tridymite in high-SiO_2 sedimentary rock at gale crater. Proc Natl Acad Sci USA 113(26):7071–7076. https://doi.org/10.1073/pnas.1607098113
5. Hippler B, Böhm H (1989) Structure investigation on sodium-nephelines. Z Kristallogr Cryst Mater 187:39–53
6. Brown WL, Cesbron F (1972) Trinepheline; a new synthetic modification in the nepheline group. Z Kristallogr Cryst Mater. https://doi.org/10.1524/zkri.1972.136.16.468
7. Klaska KH (1974) Strukturuntersuchugen an Tribymitabkommlingen. PhD Thesis, Universitat Hamburg, Germany
8. von Jarchow O, Reese HH, Saalfeld H (1966) Hydrothermalsynthesen von Zeolithen Der Sodalith-Und Cancrinitgruppe. Neues Jahrb Mineral Mh 10:289–297
9. Selker P, Bartsh HH, Klaska R (1985) Struktur Und Hydrothermalsynthesen von $NaAlSiO_4$-Modifikationen. Z Kristallogr 170:175–176
10. Kahlenberg V, Bohm H (1998) Crystal structure of hexagonal trinepheline—a new synthetic $NaAlSiO_4$ modification. Am Mineral 83:631–637
11. Vulic P, Kahlenberg V, Konzett J (2008) On the existence of a Na-deficient monoclinic trinepheline with composition $Na_{7.85}Al_{7.85}Si_{8.15}O_{32}$. Am Mineral 93(7):1072–1079. https://doi.org/10.2138/am.2008.2702
12. Balassone G, Kahlenberg V, Altomare A, Mormone A, Rizzi R, Saviano M, Mondillo N (2014) Nephelines from the Somma-Vesuvius Volcanic Complex (Southern Italy): crystal-chemical, structural and genetic investigations. Mineral Petrol 108(1):71–90. https://doi.org/10.1007/s00710-013-0290-6
13. Gregorkiewitz M (1984) Crystal structure and Al/Si-ordering of a synthetic nepheline. Bull minéral 107(3–4):499–507
14. Merlino S, Franco E, Mattia C, Pasero M, De Gennaro M (1985) The crystal structure of panunzite (natural tetrakalsilite). Neues Jahrb Mineral 7:322–328
15. Cellai D, Bonazzi P, Carpenter MA (1997) Natural kalsilite $KAlSiO_4$ with P31c symmetry: crystal structure and twinning. Am Mineral 82:276–279
16. Andou Y, Kawahara A (1984) The refinement of the structure of synthetic kalsilite. Mineral J 12(4):153–161. https://doi.org/10.2465/minerj.12.153
17. Becerro AI, Escudero A, Mantovani M (2009) The hydrothermal conversion of kaolinite to kalsilite: influence of time, temperature, and pH. Am Mineral 94(11–12):1672–1678. https://doi.org/10.2138/am.2009.3284
18. Dollase WA, Freeborn WP (1977) The structure of $KAlSiO_4$ with P63mc symmetry. Am Mineral 62:420–421
19. Gregorkiewitz M, Li Y, White TJ, Withers RL, Sobrados I (2008) The structure of "Orthorhombic" $KAlSiO_4$–O_1: evidence for Al–Si order from MAS NMR data combined with Rietveld refinement and electron microscopy. Can Mineral 46(6):1511–1526. https://doi.org/10.3749/canmin.46.6.1511
20. Khomyakov AP, Nechelyustov GN, Sokolova E, Bonaccorsi E, Merlino S, Pasero M (2002) Megakalsilite, a new polymorph of $KAlSiO_4$ from the Khibina alkaline massif, Kola Peninsula, Russia: mineral description and crystal structure. Can Mineral 40(3):961–970. https://doi.org/10.2113/gscanmin.40.3.961
21. Byrappa K, Yoshimura M (2001) Handbook of hydrothermal technology: a technology for crystal growth and materials processing. Noyes Publications, Norwich
22. Halasyamani PS, Poeppelmeier KR (1998) Noncentrosymmetric oxides. Chem Mater 10(10):2753–2769. https://doi.org/10.1021/cm980140w
23. Tran TT, Yu H, Rondinelli JM, Poeppelmeier KR, Halasyamani PS (2016) Deep ultraviolet nonlinear optical materials. Chem Mater 28(15):5238–5258. https://doi.org/10.1021/acs.chemmater.6b02366

24. Winkler HGF (1947) On the synthesis of nepheline. Am Mineral 32:131–136
25. Iwasaki F, Iwasaki H (2002) Historical review of quartz crystal growth. J Cryst Growth 237:820–827. https://doi.org/10.1016/S0022-0248(01)02043-7
26. Thompson RJ (2007) Crystal clear: the struggle for reliable communications technology in World War II. IEEE Press, Wiley-Interscience, Hoboken
27. Becker P (1998) Borate materials in nonlinear optics. Adv Mater 10(13):979–992. https://doi.org/10.1002/(SICI)1521-4095(199809)10:13%3c979::AID-ADMA979%3e3.0.CO;2-N
28. Terry RJ, Vinton D, McMillen CD, Kolis JW (2018) A cesium rare-earth silicate $Cs_3RESi_6O_{15}$ (RE=Dy–Lu, Y, In): the parent of an unusual structural class featuring a remarkable 57 Å unit cell axis. Angew Chem Int Ed 57(8):2077–2080. https://doi.org/10.1002/anie.201708798
29. McMillen DC, Kolis WJ (2016) Hydrothermal synthesis as a route to mineralogically-inspired structures. Dalton Trans 45(7):2772–2784. https://doi.org/10.1039/C5DT03424H
30. Fulle K, Sanjeewa LD, McMillen CD, Kolis JW (2017) Crystal chemistry and the role of ionic radius in rare earth tetrasilicates: $Ba_2RE_2Si_4O_{12}F_2$ (RE = Er^{3+}–Lu^{3+}) and $Ba_2RE_2Si_4O_{13}$ (RE = La^{3+}–Ho^{3+}). Acta Crystallogr B 73(5):907–915. https://doi.org/10.1107/S2052520617009544
31. Mann JM, McMillen CD, Kolis JW (2015) Crystal chemistry of alkali thorium silicates under hydrothermal conditions. Cryst Growth Des 15(6):2643–2651. https://doi.org/10.1021/cg5017164
32. Lee C-S, Lin C-H, Wang S-L, Lii K-H (2010) $[Na_7UIVO_2(UVO)_2(UV/VIO_2)_2Si_4O_{16}]$: a mixed-valence uranium silicate. Angew Chem Int Ed 49(25):4254–4256. https://doi.org/10.1002/anie.201001095
33. Terry RJ, McMillen CD, Chen X, Wen Y, Zhu L, Chumanov G, Kolis JW (2018) Hydrothermal single crystal growth and second harmonic generation of Li_2SiO_3, Li_2GeO_3 and $Li_2Si_2O_5$. J Cryst Growth 493:58–64. https://doi.org/10.1016/j.jcrysgro.2018.02.028
34. Bruker (2015) APEX3. Bruker AXS, Madison
35. Sheldrick GM (2015) Crystal structure refinement with SHELXL. Acta Crystallogr C 71(1):3–8. https://doi.org/10.1107/S2053229614024218
36. Momma K, Izumi F (2011) VESTA 3 for three-dimensional visualization of crystal, volumetric and morphology data. J Appl Crystallogr 44(6):1272–1276. https://doi.org/10.1107/S0021889811038970
37. Tuttle OF, Smith JV (1958) The nepheline–kalsilite system; II, phase relations. Am J Sci 256(8):571–589. https://doi.org/10.2475/ajs.256.8.571
38. Bannister FA, Hey MH (1931) A chemical, optical, and X-ray study of nepheline and kaliophilite. Mineral Mag 22(134):569–608. https://doi.org/10.1180/minmag.1931.022.134.03
39. Shannon RD (1976) Revised effective ionic radii and systematic studies of interatomic distances in halides and chalcogenides. Acta Crystallogr A 32(5):751–767. https://doi.org/10.1107/S0567739476001551
40. Kawahara A, Andou Y, Marumo F, Okuno M (1987) The crystal structure of high temperature form of kalsilite ($KAlSiO_4$) at 950°C. Mineral J 13(5):260–270. https://doi.org/10.2465/minerj.13.260
41. Cellai D, Gesing T, Wruck B, Carpenter AM (1999) X-ray study of the trigonal → hexagonal phase transition in metamorphic kalsilite. Am Mineral. https://doi.org/10.2138/am-1999-11-1223
42. Simmons WB, Peacor DR (1972) Refinement of the crystal structure of a volcanic nepheline. Am Mineral 57(11–12):1711–1719
43. Foreman N, Peacor DR (1970) Refinement of the nepheline structure at several temperatures. Z Kristallogr Cryst Mater 132(1–6):45–70. https://doi.org/10.1524/zkri.1970.132.16.45
44. Buerger MJ, Klein GE, Donnay G (1954) Determination of the crystal structure of nepheline. Am Mineral 39:805–818
45. Antao SM, Hassan I (2010) Nepheline: structure of three samples from the Bancroft area, Ontario, obtained using synchrotron high-resolution powder X-ray diffraction. Can Mineral 48(1):69–80. https://doi.org/10.3749/canmin.48.1.69
46. Hassan I, Antao SM, Hersi AAM (2003) Single-crystal XRD, TEM, and thermal studies of the satellite reflections in nepheline. Can Mineral 41(3):759–783. https://doi.org/10.2113/gscanmin.41.3.759
47. Henderson CMB, Roux J (1977) Inversions in sub-potassic nephelines. Contrib Mineral Petrol 61(3):279–298. https://doi.org/10.1007/BF00376702
48. Henderson CMB, Thompson AB (1980) The low-temperature inversion in sub-potassic nephelines. Am Mineral 65:970–980
49. Schneider H, Flörke OW, Stoeck R (1994) The $NaAlSiO_4$ nepheline–carnegieite solid-state transformation. Z Kristallogr Cryst Mater 209(2):113–117
50. Liebau F (1985) Structural chemistry of silicates: structure, bonding, and classification. Springer, Berlin
51. Gatta GD, Angel RJ, Carpenter MA (2010) Low-temperature behavior of natural kalsilite with P31c symmetry: an in situ single-crystal X-ray diffraction study. Am Mineral 95(7):1027–1034. https://doi.org/10.2138/am.2010.3478
52. Gatehouse BM (1989) Structure of $CsAlTiO_4$—a compound with TiO_4 tetrahedra. Acta Crystallogr C 45(11):1674–1677. https://doi.org/10.1107/S010827018900418X